

# Effect of Colloidal Stability of Diamond Nanoparticles on the Ni-W/Diamond Electro-co-deposition Composite Coatings and Evaluation of Corrosion Resistance

Han-Tao Wang<sup>1</sup>, Jee-Ray Wang<sup>2</sup>, Ming-Der Ger<sup>3,\*</sup>, Kung-Hsu, Hou<sup>4,\*</sup>

<sup>1</sup> School of Defense Science, Chung Cheng Institute of Technology, National Defense University

<sup>2</sup> Department of Automation Engineering & Institute of Mechatronic, Chienkuo Technology University, Changhua, Taiwan

<sup>3</sup> Department of Chemistry and Materials Engineering, Chung Cheng Institute of Technology, National Defense University

<sup>4</sup> Department of Power Vehicle and Systems Engineering, Chung Cheng Institute of Technology, National Defense University

\*E-mail: [khoucloud@gmail.com](mailto:khoucloud@gmail.com), [khou@ndu.edu.tw](mailto:khou@ndu.edu.tw), [mingderger@gmail.com](mailto:mingderger@gmail.com)

Received: 10 November 2015 / Accepted: 22 December 2015 / Published: 1 February 2016

---

Ni-W/diamond composite coatings can be produced by co-deposition of nickel-tungsten matrix with micro-sized diamond particles under direct current (DC) from aqueous citrate electrolytes in which diamond particles are dispersed. The present study investigated the effect of pH value on the dispersion stability of diamond particles in a suspension and deposition behavior of diamond particles in composite electroplating. Increasing the electrolyte pH caused an increase of co-deposited diamond particles within the present experimental range. At pH = 8.5, the maximum volume percentage of the embedded diamond particles in composite coating was obtained. In addition, the current efficiency and deposition rate increased. The tungsten content of the composite coating, however, decreased with increasing pH value of the plating bath during electroplating process. The anodic polarization curves were implemented to evaluate the corrosion behavior of Ni-W alloy and Ni-W/diamond composite coatings. The analysis shows that Ni-W/diamond composite coating has better corrosion resistance.

---

**Keywords:** Ni-W, diamond, composite coating, electro-co-deposition, corrosion resistance.

## 1. INTRODUCTION

Due to the diamond with marvelous mechanical, electrical and tribological properties, including high degree of hardness, good electrical insulation, low friction coefficient and chemical

attack-inertness, diamond has aroused considerable technological interest. Its application as an engineering material, however, has been limited in range mainly because of its scarcity, price and relative difficulty in deformation [1]. In response to such a characteristic, diamond-based composites have been developed and widely used in industries. The co-electrodeposition technique, through which ceramic or organic particles are simultaneously deposited with metal ions on a substrate, has been extensively used over the past few decades [2–6].

By blending metallic and nonmetallic second phase materials, this technique enables coatings to be produced with new and unique characteristics. We should be aware that particle size, size distribution, particle density and shape, plating uniformity and the properties of the matrix metal can exert influence on the properties of electroplated composite coatings. The matrix of a composite deposit could be made up of a metal [7–11] or an alloy [12–15]. Recently, electrodeposited nickel-tungsten (Ni-W) alloys have been developed in place of the environmentally hazardous hexavalent hard chromium coating. However, it is less hard than the traditional chromium coating [16]. As has been widely known, incorporating micro- or nano-sized particles into coatings can enhance the hardness, corrosion, and wear properties of coatings. According to Burkat et al (17), adding pure detonation synthesis nano-diamonds into nickel- or iron-based plating would be increase the micro-hardness (about 2-3.5 times) and the wear-resistance (about 3-6 times), and decrease porosity (about 3-4 times). Mazaheri et al. [18] indicated that in contrast to the deposit Ni-P coatings, Ni-P/nano-diamond composite coatings had higher corrosion and greater hardness. The study by Habib et al. [19] demonstrated that incorporation of dispersed diamond nanoparticles significantly improved corrosion resistance of Ni-P coatings. So far, however, there has been no technique applicable to electroplating of Ni-W/diamond composite coatings.

In the process of co-electrodeposition, solid inert particles are suspended in a conventional plating electrolyte and captured in the growing metal film. Obviously, the properties of the composite coatings depend to a large extent on the incorporation percentage of particles and uniform distribution of inert particles in the metal matrix. Ogihara et al. [13], who prepared Ni-B/diamond films with high hardness by using conventional electrodeposition, concluded that composite films with higher diamond content and larger diamond particles showed higher film hardness. As poor wettability can be detrimental to the properties [20], there is difficulty depositing sub-micron particle over 10 vol.-%. Thus, surfactants have been extensively added to an electrolyte bath to improve the content of particles in the composite coatings [11, 21-25]. Another, surfactants can change surface charge of the particles and decrease their tendency to agglomeration on the other hand. The absorption of anionic or cationic surfactant on the surface of particles can be contributive to particle stability on the electrolyte, thus leading to an increase of the strength of the surface charge on the particles. Particles with high zeta potential (absolute value) tend to repel each other and resist agglomeration. The absorption of cationic surfactant on particles might give a more positive charge to particle surfaces, and therefore increases the forces of electrostatic attraction between the particles and the negatively charged cathode. A higher content of particles will be co-deposited in the matrix, accordingly. Excessive surfactants, however, can reduce the cathode area and increase deposit brittleness [26].

The Zeta potential of particles can be changed by simply adjusting the pH of the system. As a result, the pH of the electrolyte plays an important role in the process of plating. Lee et al. [27]

investigated the effect of pH of the plating bath on the deposition behaviors of Ni/SiC composite coating layers. The study found that with the increasing pH value by adding alkali, the Zeta potential of a particle in the solution became more negative. Thus, the deposition of SiC can be increased by increasing the pH of the plating bath. In addition, there has been extensive research on the effect of pH on the dispersion stability of particles in the solution [28-32]. It can be inferred, consequently, that the pH of the plating will significantly affect the amount of inert particles which are co-deposited into the composite coating. The present study examined the effects of the pH of the plating bath on the Zeta potential and dispersion stability of diamond particles in a suspension. Also under investigation was the influence of pH on co-deposition behavior of diamond particles in composite electroplating and the corrosion resistance properties of the Ni/W/diamond composite coatings.

## 2. EXPERIMENTAL

A direct current electroplating method was used to co-deposit Ni-W/diamond coatings. Table 1 shows the plating bath composition and operational parameters.

**Table 1.** Bath composition and electroplating conditions.

Bath composition		electroplating conditions	
NiSO <sub>4</sub> ·6H <sub>2</sub> O	0.06 M	pH	5.5, 7, 8.5, 10
Na <sub>2</sub> WO <sub>4</sub>	0.14 M	Temperature	75 °C
Na <sub>3</sub> C <sub>6</sub> H <sub>5</sub> O <sub>7</sub>	0.4 M	Current density	10 A/dm <sup>2</sup>
NH <sub>4</sub> Cl	0.5 M	Stirring speed	180 rpm
Diamond particle	1 g/L	Plating time	120 min

All the chemicals were of analytical grade quality. The average size of the diamond particles (Taiwan union Abarasives Co.) used in the experiment was about 500 nm with a purity of 99.0%. The solution pH value was adjusted by the diluted sulfuric acid and ammonia. A stainless steel sheet with an area of 33mmx50mm was used as the cathode. The solution containing diamond particles was ultrasonically dispersed for 10 min before the co-deposition.

A dispersion stability analyzer (L.U.M. GmbH, LUMSizer) was used under centrifugation forces to examine the effect of the pH on the sedimentation behavior of diamonds in the electrolyte solution. The light transmission was measured at various radial positions of the sample *r* and at various centrifugation times *t* over the entire sample length simultaneously. The transmission profiles can be converted into sedimentation-time curves. These curves represent the motion of the boundary between the clear phase (electrolyte) and the sediment toward the cuvette bottom as a function of time. The slope in the sedimentation curve refers to the sedimentation rate. The samples of 100 ppm diamond electrolyte solution at various pH values were ultrasonically dispersed for 3 min and then subjected to centrifugation in the quadratic polystyrene tube of 10×10 mm<sup>2</sup>. Centrifugation experiments were conducted at 200 rpm corresponding to 116g centrifugal acceleration for 40 min at room temperature.

Diamond dispersion with pH values of 5.5, 7, 8.5 and 10 was respectively used in centrifugal experiments. The Zeta potential and particle size distribution of the dispersed diamond aqueous solution were determined by the micro-electrophoretic apparatus Zeta Plus (Brockhaven Instruments Corporation, JUSA), where the dynamic light scattering technique was applied for determination of these quantities. In the experiment, 100ppm diamond was dispersed in nonionic aqueous solutions and was treated in an ultrasonic bath for 3 min in order to break up aggregates in the suspension. The suspension was left for 1 h and then the pH of suspension, zeta potential, effective diameter and sedimentation rate were determined.

A scanning electron microscopy (SEM, Jeol model JSM-6500) was used to observe the surface morphology and microstructure of the coatings. The average size of the embedded particles was determined by SEM with the image analysis software (Image J). Compositional analysis of W-content and Al content in the coatings was obtained by applying Electron Probe X-ray Microanalyzer (EPMA). The volume percent of diamond was then determined by using the previously measured diamond content.

A conventional three-electrode cell was applied for the electrochemical experiments. The counter electrode was platinum electrode, whereas the reference electrode was a saturated calomel electrode (SCE). The working electrode was Ni-W alloy and Ni-W/diamond composite coating with an expressed area of 1 cm<sup>2</sup>. Electrode solutions were prepared with analytical grade reagents and distilled water. Electrochemical measurements were conducted at 25°C using CHI 660 electrochemical workstation. The anodic polarization curves in 0.5 g/L NaCl solution were measured through linear potential scan from 0.1 to 0.9 volt by scanning the potential at 0.5 mV/s. Tungsten content of all test samples ranged between 42 wt.% and 45 wt.% and diamond particle content was about 21 vol.%.

### 3. RESULTS AND DISCUSSION

The researchers implemented a dispersion stability analyzer to quantitatively evaluate the variation of diamond dispersion with time. This was meant to examine the effect of pH on dispersion stability of diamond particles in electrolyte solution. The principle of centrifugal sedimentation is based on the Stokes' Law, a formula developed for determining the sedimentation rate. According to it, a particle moving through viscous liquid attains a constant velocity or sedimentation rate. The following is the equation for Stokes' law of sedimentation:

$$V = \frac{2r^2(\rho_p - \rho_s)g}{9\mu_s} \quad (1)$$

where  $V$  is sedimentation velocity,  $r$  is the particle diameter,  $\rho_p$  is particle density,  $\rho_s$  is liquid density,  $g$  is the gravity acceleration, and  $\mu_s$  is the liquid viscosity. The result of dispersion stability analysis for the diamond solutions with various pH values was demonstrated in Fig. 1. The relative centrifugal force was 110 g.

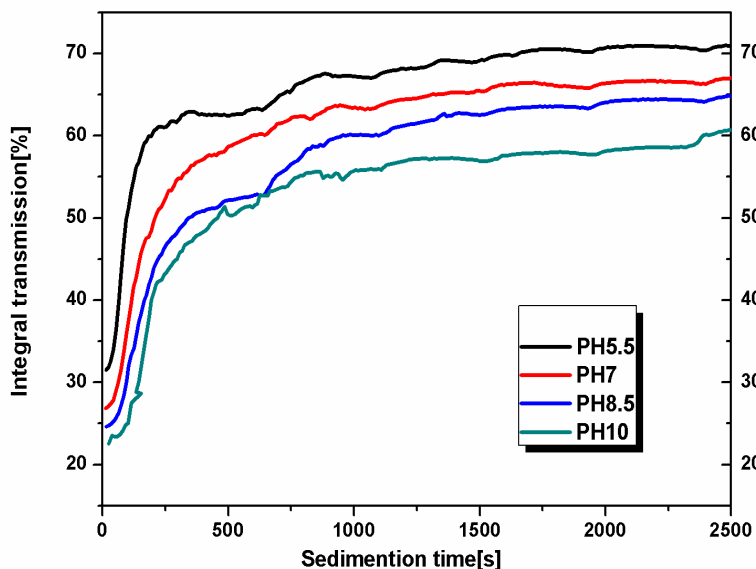


**Figure 1.** The results of dispersion stability analysis for diamond solutions: the lower the transmission is, the better the dispersion of diamond becomes. The pH values used respectively are, from top (worst) to bottom (best), pH5.5, pH7, pH8.5, and pH10.

The curves, from top (worst) to bottom (best), respectively correspond to the electrolyte pH values of 5.5, 7, 8.2, and 10. Fig 1 shows the integral transmission decreases as pH increases. It manifests that the lower the integral transmission is, the better the dispersion of diamond is. Obviously, the best dispersion of diamond particles is obtained from an electrolyte of pH 10.

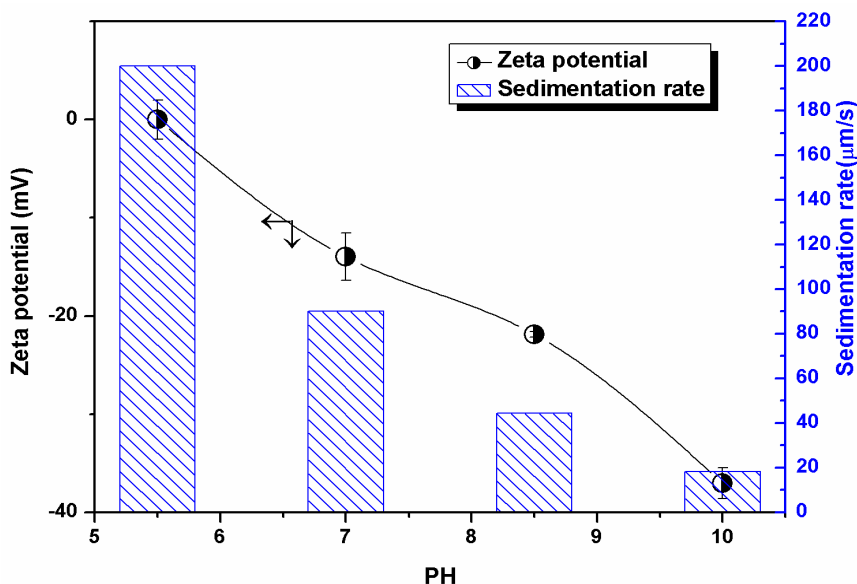


**Figure 2.** Zeta potential and sedimentation rate of the diamond particles with pH of solution.

The effect of pH on zeta potential of diamond particles, which is implemented to clarify the effect of pH on the dispersion stability of diamond particles, is shown in Fig. 2. Fig. 2 shows that the

potential of diamond particles in aqueous solution decreases with increasing pH value. The isoelectric point (IEP) is defined as the pH at which the surface is neutrally charged. As indicated by Fig. 2, the diamond surface approaches the IEP (the point of zero Zeta potential) at a pH around 5.5. According to Lee et al., [33] the zeta potential for diamond particles decreases linearly with pH, and the point of zero charge (pzc) pH appears to be 3.2. The discrepancy between IEP obtained in the present study (5.5) and the value reported in literature [32] may be attributed to the diversity of functional groups on diamond surface resulting from the diversity of precursor compositions and purification method. The Zeta potential is around -37.06 mV as pH goes down to 10. Suspensions that have a measured zeta potential above 30 mV or below are regarded stable as these particles maintain their repulsive forces during dispersion [34]. This is point to the fact that diamond particles are stable at a solution of pH 10. Therefore, there is a good agreement between the dispersion stability analysis and the Zeta potential results. Fig. 2 also demonstrates that the sedimentation of diamond particles becomes faster as the suspension pH decreased. This indicates that, by enhancing the rate of direct particle-to-particle interaction, the pH affects the rate and degree of the agglomeration.

The relationship between the solution pH value and average diameters of diamond particles, calculated from light scattering formula, is given in Fig. 3.

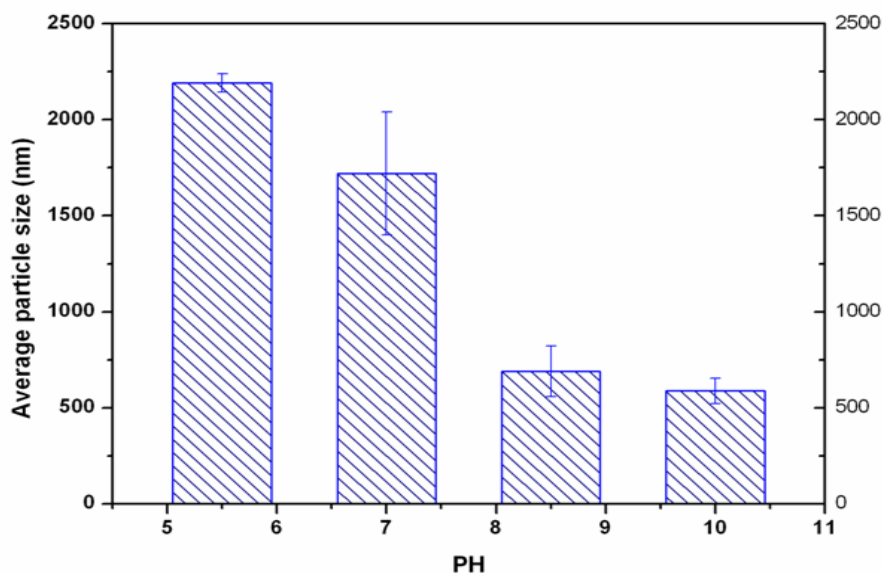


**Figure 3.** Influence of suspension pH value on diamond particle size

The average particle size obtained from an aqueous solution of pH=5.5 is approximately 2200 nm, which is 4.4 times larger than the average particle size of pristine diamond. It implies that the diamond particles are highly agglomerated at pH 5.5. As pH value goes up to 7, 8.5, and 10, the average particle size respectively reduces to 720, 652, and 550 nm. The average particle size obtained from an aqueous solution of pH=10 obviously is close to the actual diameter of diamond particles (500nm), suggesting a good dispersion stability of suspension. Good concurrence of the IEP maximum of the effective diameter and the sedimentation rate can be seen from Fig. 2 and Fig.3. The zeta

potential curves makes it clear to us that, electric repulsion between particles is quite small around pH level 5.5 (IEP), where zeta potential is quite near zero. When the extent of the repulsive energy is smaller compared to the Van der Waals attraction energy, the dispersion becomes unstable, thus giving rise to the aggregation of particles. Due to this agglomeration, large particles are formed, which can be proved by particle size measurement. According to Stokes law, the rate of sedimentation of a particle is in right proportion to the square of its diameter and a larger particle would sediment faster, accordingly. As a result, the sedimentation of diamond particles is faster as the suspension approaches pH-5.5 from the basic pH range.

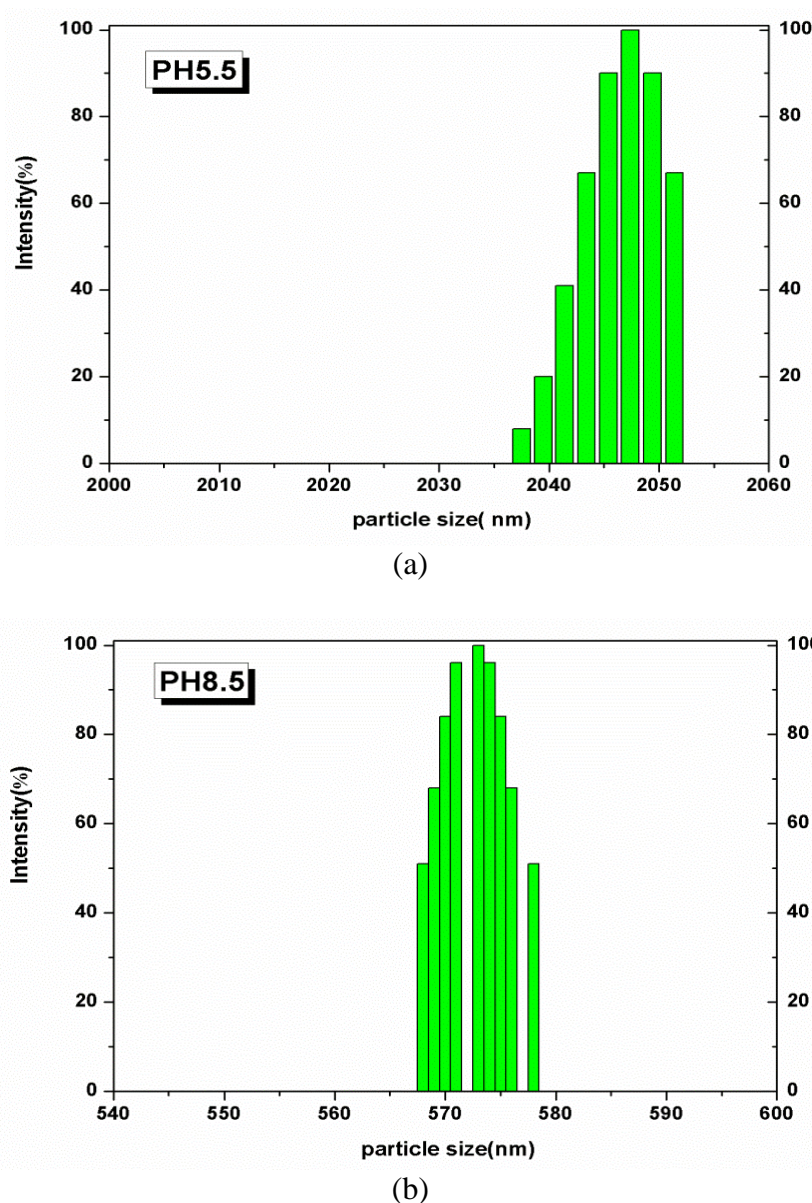


**Figure 4.** Particle size distribution of diamond particles prepared in a de-ionic water solution with concentration of  $1 \text{ gL}^{-1}$ , determined by dynamic light scattering: (a) pH = 5.5; (b) pH = 8.5

Fig. 4 compares the particle size distribution of diamond in the aqueous solutions at pH=5.5 and 8.5. The result is in agreement with the average particle size mentioned above. The particle size

distribution for low pH (5.5) is broader than that for high pH (8.5). This can be explained in terms of agglomeration.

Fig. 5 shows the cross-sectional SEM images of Ni-W/diamond composite coatings deposited from electrolytes with various pH values.

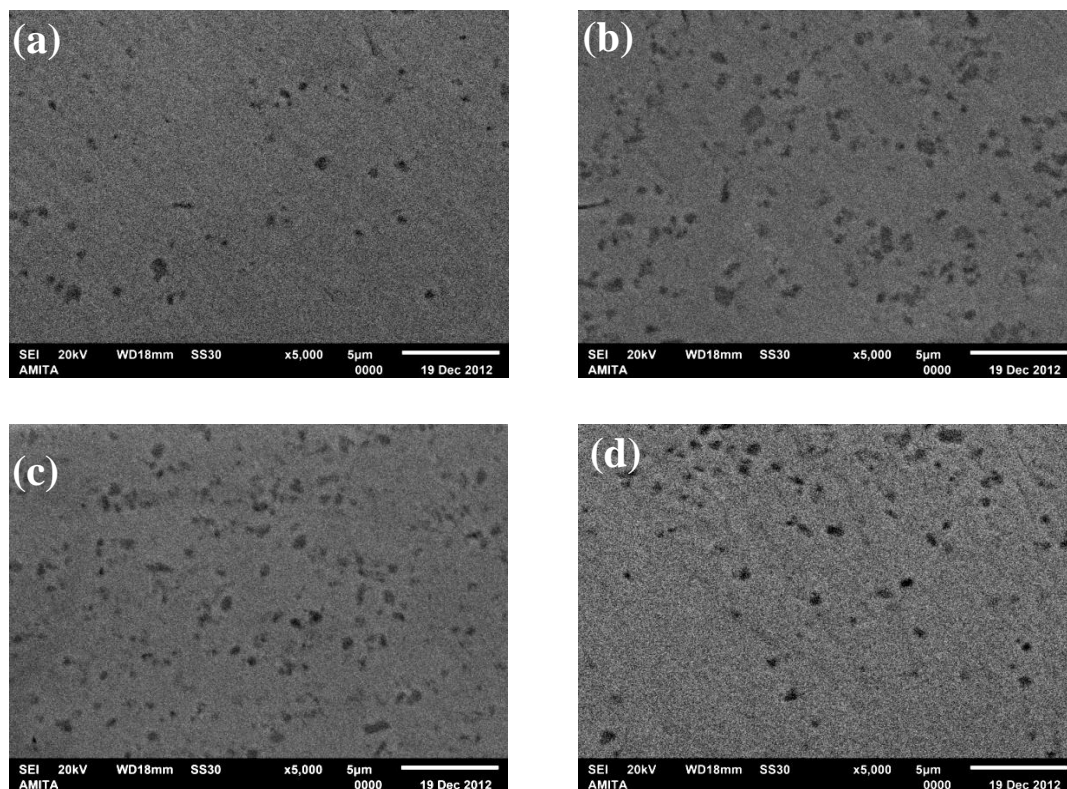


**Figure 5.** SEM micrographs of the cross section (X5K) and of Ni-W/diamond composite coatings obtained at various pH values: (a) pH =5.5; (b) pH=7; (c) pH=8.5; (d) pH=10

All the coatings are crack-free. Furthermore, it demonstrates the content and distribution of diamond particles in the composite coating. One thing worth noting is that as far as the case of the acid bath (pH-5.5) is concerned, the distribution of the diamond particles in the nickel-tungsten matrix is non-uniform and diamond particle content is about 11.4 vol.-%(Fig. 5a). This mainly results from the poorest dispersion stability as well as the fastest sedimentation rate of diamond particles in this acidic electrolyte. In contrast, the film plated from the basic bath shows a more uniform distribution of particles within the metal matrix (Fig. 5b and c). The maximum incorporation of 21.2 vol.-% diamond is found in the coating obtained from the electrolyte of pH 8.5. It can be found that the volume percentage of diamond powder in the coatings increases with increasing pH of the plating solution in the pH range between 5.5 and 8.5. Nevertheless, the volume percent of diamond particles decreases to 13 vol. -% pH=10 (Fig. 5d). Interestingly, the Ni-W/diamond composite coating obtained from the electrolyte of pH 8.5 is significantly thicker than that obtained from the electrolyte of pH 5.5 (Fig. 6). According to the cross-section view of Ni-W/diamond composite coating obtained from the electrolyte of pH 8.5 (Fig. 6a), the diamond particles are not uniformly distributed along the surface normal

direction, i.e. the co-deposition of diamond is found to be low near the substrate and high near the surface of the composite coating layer.

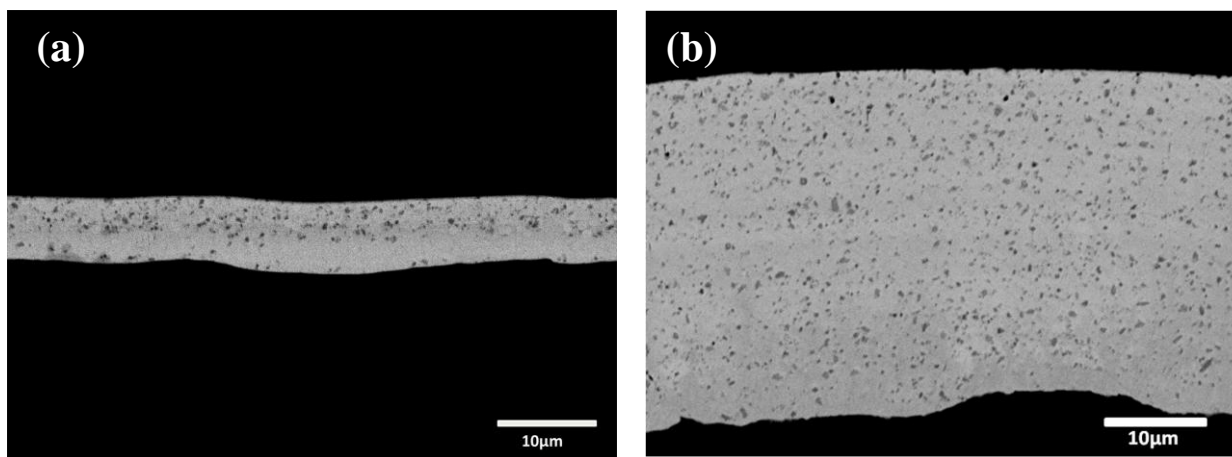


**Figure 6.** SEM micrographs of the cross section (X2K) and of Ni-W/diamond composite coatings deposited from electrolytes with various pH values: (a) pH =5.5; (b) pH=8.5

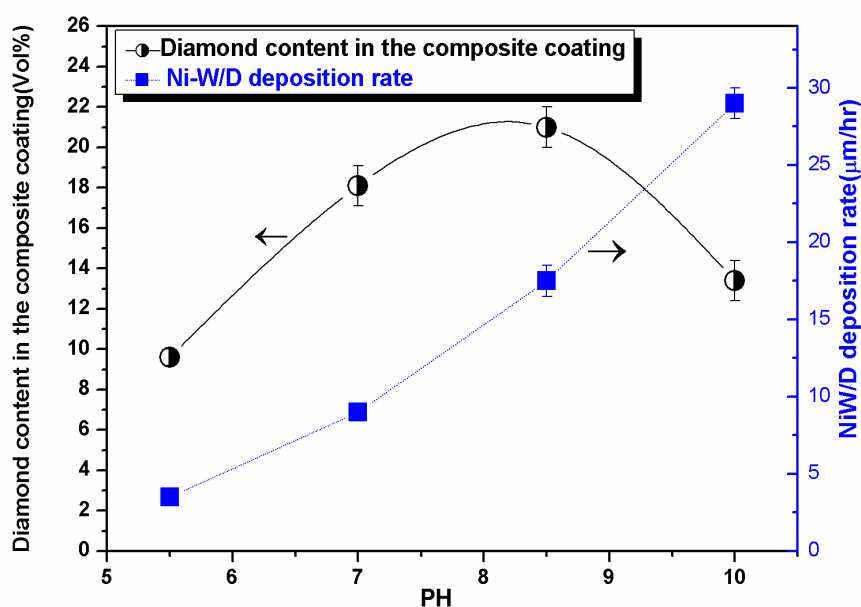


**Figure 7.** Variation of deposition rate and diamond content in the coating with pH value of electrolyte

This results from preferential deposition of nickel during the initial stage of electrolyte plating without incorporating diamond particles due to the low electrophoretic velocity of agglomerated diamond particles. To sum up, the quality of composites and deposition rate can be significantly improved with the alkaline bath.

Fig. 7 shows variation of deposition rate and diamond content in the coating with pH value of electrolyte. Obviously, the deposition rate of the coating increased in right proportion to pH value of

the plating bath. The maximum deposition of 29  $\mu\text{m/hr}$  is found in the bath of pH 10. This is almost eight times the deposition rate found in the rate of the acidic bath with a pH of 5.5 (3.5  $\mu\text{m/hr}$ ). On the other hand, the diamond content in the coating tends to increase with increasing pH value as the pH increases from 5.5 to 8.5. However, where the pH is between 8.5 and 10, there is evidently a decrease of particle incorporation. A maximum incorporation of about 21.1 vol. -% diamond is obtained from this electrolyte of pH 8.5. This conforms to the findings by Narasimman et al.[35], who studied the effect of silicon carbide (SiC) concentration and bath operating parameters on the volume percentages and deposition rate of Ni/SiC coatings obtained with the two kinds (micro- and nano-sized of SiC particles). That co-deposition of SiC increases with increasing pH value is explained as electrophoresis phenomenon resulting from the formation of an ionic cloud around the SiC particle [27]. It is known that most colloidal particles in aqueous solution are in charged state. As a consequence, a charged particle suspended in an electrolyte solution tends to be surrounded by an ionic cloud. It was reported that the diamond particles with negative surface charge could firstly absorb  $\text{Ni}^{2+}$  ions, and then diamond particles were attracted electronically to the cathode [33]. As the Zeta-potential of particles decreases with increasing pH, the size of the ionic cloud-surrounded particles increases with increasing pH. It enhances the second stage of Guglielmi model, which concerns about the radiation of ionic cloud and strong absorption of particles. As a result, co-deposition of particles increases with increasing pH value. Nevertheless, at higher pH value (10), the enhancement of metal deposition rate, which is caused by an increase in pH, exceeds the promotion effect of particle incorporation, thus resulting in a decrease of the particle content.

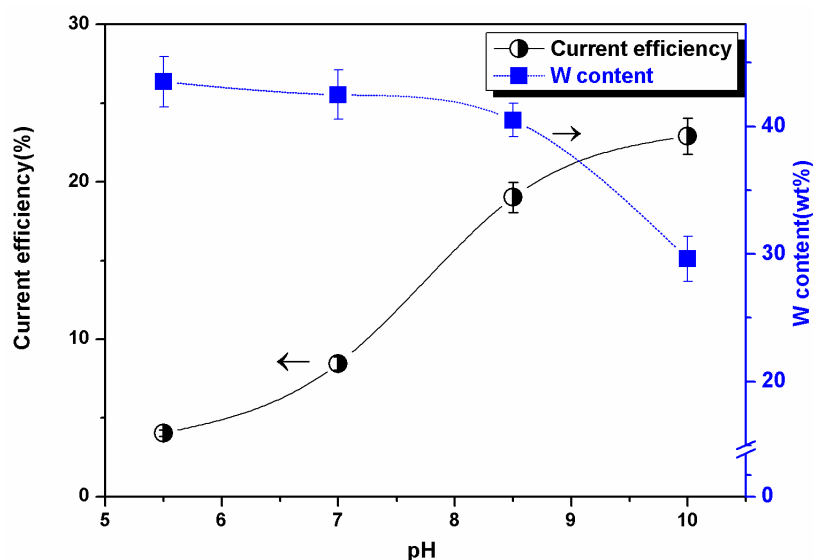


**Figure 8.** Variation of current efficiency and tungsten content with pH value of electrolyte

Fig 8 shows the effect of pH on the current efficiency of co-electrodeposition. It reveals that the current efficiency decreases as the pH value of the plating bath increases. The dependence of cathodic current efficiency on pH is approximately linear, which is shown by Fig. 8. Hydrogen evolution always occurs as a side reaction in electroplating process. It was reported that reduction of nickel ions from dilute solution was highly dependent on the pH value. At low pH value, hydrogen tends to evolve

because of the small hydrogen evolution over potential. When the pH value of the bath is increases, the equilibrium sufficient potential is displaced to enable nickel to deposit [36]. Due to less hydrogen evolution at higher pH value, more metal is deposited and the current efficiency for metal deposition increases with pH value. Fig. 8 also indicates that the tungsten content of the composite coating decreases with increasing pH value of the plating bath. This result can be explained by the mechanism proposed by Younes et al. Deposits here are a lot of papers for the mechanisms of W and Ni co-deposition [37-43]. However, the true mechanism of co-electrodeposition of Ni/W still remains unclear. According to Younes et al [40, 42-43], W is electrodeposited from a mixed complex  $[(Ni)(WO_4)_2(H)_2(Cit)]^{2-}$ , which serves as the precursors for deposition of Ni/W alloys. As the pH increases, the concentration of this ternary complex decreases, thus leading to lower concentration of W in the alloy.

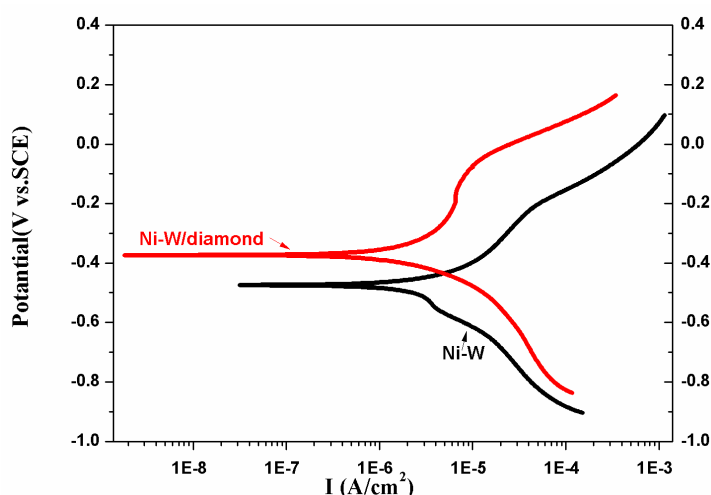


**Figure 9.** Anodic polarization curves of Ni–W alloy and Ni–W/diamond composite coating

Fig. 9 shows the potential dynamic polarization of Ni-W alloy and N-W diamond composite coating in 0.5 mode/L NaCl solution. Compared to a Ni-W alloy coating, Ni/W diamond composite coating is found to have excellent corrosion resistance. As regards the Ni-W diamond composite coating, the corrosion potential obtained from the polarization curves is  $-0.369$  V; the Ni-W alloy,  $-0.469$  V. The corrosion potential of Ni-W/diamond composite coating has lower chemical activity than the Ni-W alloy coating does. As a result, it possesses better chemical stability in the external environment. Moreover, the corrosion current value of the Ni-W/diamond composite coating ( $I_{\text{corr}} = 1.738 \times 10^{-6} \text{ A/cm}^2$ ) is comparatively smaller than that of Ni/W alloy coating ( $I_{\text{corr}} = 2.559 \times 10^{-6} \text{ A/cm}^2$ ). This means that the Ni-W diamond composite coating has better corrosion resistance than the Ni-W alloy coating. Furthermore, anode tafel slope of Ni–W/diamond composite coating is sharper than that of Ni–W alloy coating. The slope of the former is  $0.5 \text{ mv/dec}$ , and the latter is  $0.3 \text{ mv/dec}$ . It means that Ni–W/diamond composite coating has passivation phenomenon in the beginning of corrosion process.

Based on the results, we can conclude that incorporation of diamond particles improves corrosion resistance of the coating. It can be attributed to the following reasons. First, diamond particles isolate the matrix from the corrosion medium, decrease the exposed area of Ni/W matrix as well as inhabited preferential corrosion sites, and inhibit the solution penetrating the coatings. Second, as diamond particles have a low level of electronic conductivity and are uniformly dispersed in the composite coating, they distract the corrosion current and result in a decrease of corrosion speed [44-46]. Third, the diamond particles acting as inert physical barriers to the initiation and development of defect corrosion are embedded in the Ni-W matrix and filled in crevices, gaps and micron holes. This enables them to improve the corrosion resistance of the coating [47-52].

#### 4. CONCLUSION

Micro-sized diamond particles were co-deposited with nickel-tungsten under direct current (DC) from aqueous citrate electrolytes in which diamond particles were dispersed and the effect of pH value of plating bath on the deposition behaviors of Ni-W/diamond composite coatings was investigated. The present study presents the following conclusions:

1. The diamond particles become more negative in the Zeta potential as the pH of the plating bath increases from 5.5 to 10. It reduces the agglomeration and sedimentation rate of diamond particles on the one hand, and enhances the dispersion stability of particles in the plating bath on the other hand.
2. Increasing the pH of the plating bath within the present experimental range always increases the co-deposition of diamond particles and leads to the production of composite coatings with enhanced distribution of embedded diamond particles in Ni-W matrix. The maximum volume percentage (about 21.1 vol.-%) of the embedded diamond particles in composite coating is obtained from the electrolyte with pH 8.5. Increasing bath pH to 10, however, decreases the volume percentage of the embedded diamond particles in composite coating.
3. The co-deposition behavior is also influenced by the pH value of the plating bath. As a result, the current efficiency and deposition rate increases the tungsten content of the composite coating, however, decreases with increasing pH value of the plating bath.
4. In accordance with anodic polarization curves, Ni/W diamond composite coating has better corrosion resistance than the Ni-W alloy coating.

#### References

1. P. W. May, *Phil. Trans. R. Soc. A*, 358 (2000) 473-495.
2. G. Parida, D. Chaira, M. Chopkar and A. Basu, *Surf. Coat. Technol.*, 205 (2011) 317-346.
3. N. S. Qu, K. C. Chan and D. Zhu, *Scripta Mater.*, 2004, 50 (2004) 1131-1134.
4. M. Srivastava, V. K. W. Grips and K. S. Rajam, *Mater. Lett.*, 62 (2008) 3487-3489.
5. I. Garciaa, J. Fransaera and J. P. Celisa, *Surf. Coat. Technol.*, 148 (2001) 171-178.
6. A. HOVESTAD and L. J. J. JANSSEN, *J. Appl. Electrochem.*, 25 (1995) 519-527.

7. V. H. Nguyen, T. N. Hoang, N. P. Nguyen, S. C. Kwon, M. Kim and J. Y. Lee, *T. Nonferr. Metal. Soc.*, 19 (2009) 975-978.
8. Y. Y. Wei, W. P. Li, H. C. Liu, Y. Z. Liu. and L. Q. Zhu, *Int. J. Miner. Metall. Mater.*, 19 (2012) 72-76.
9. X. He, Y. Wang, X. Sun and L. Huang, *J. Nanosci. Nanotechnol.*, 4 (2012) 48-52.
10. T. Tsubota, S. Tanii, T. Ishida, M. Nagata and Y. Matsumoto, *Diamond Relat. Mater.*, 14 (2005) 608-612.
11. N. K. Shrestha, T. Takebe and T. Saji, *Diamond Relat. Mater.*, 15 (2006) 1570–1575.
12. M. Pushpavanam, H. Manikandan and K. Ramanatha, *Surf. Coat. Technol.*, 14 (2007) 6372-6379.
13. H. Ogihara, M. Safuan and T. Saji, *Surf. Coat. Technol.*, 212 (2012) 180–184.
14. Y. Wang, Q. Zhou, K. Li , Q. Zhong, and Q. B. Bui, *Ceram. Int.*, 41, (2015) 79–84.
15. Y. L. Shi, Z. Yang, M. K. Li, H. Xu and H. L. Li, *Mater. Chem. Phys.*, 87 (2004) 154-161.
16. Y. Boonyongmanerat, K. Saengkiattiyut, S. Saenapitak, and S. Sangsuk, *Surf. Coat. Technol.*, 203 (2009) 3590-3594.
17. G. K. Burkat, T. Fujimura, V. Y. Dolmatov, E. A. Orlova and M. V. Veretennikova, *Diamond Relat. Mater.*, 14 (2005) 1761-1764.
18. H. Mazaheri and S. R. Allahkaram, *Appl. Surf. Sci.*, 258 (2012) 4574-4580.
19. A. S. Habib and E. Moosa, *Corros. Sci.*, 77 (2013) 185-193.
20. H. Gül, F. Kılıç, M. Uysal, S. Aslan, A. Alp and H. Akbulut, *Appl. Surf. Sci.*, 258 (2012) 4260-4267.
21. L. Chen, L. Wang, Z. Zeng and J. Zhang, *Mater. Sci. Eng. A*, 434 (2006) 319-325.
22. C. Guo, Y. Zuo, X. Zhao, J. Zhao and J. Xiong, *Surf. Coat. Technol.*, 202 (2008) 3385-3390.
23. M. D. Ger, *Mater. Chem. Phys.*, 87 (2004) 67–74.
24. R. Sen, S. Bhattacharya, S. Das and K. Das, *J. Alloys Compd.*, 489 (2010) 650-658.
25. E. Rudnik, L. Burzyńska, Ł. Dolasiński and M. Misiak, *Appl. Supercond.*, 256 (2010) 7414-7420.
26. L. M. Chang, M. Z. An, H. F. Guo and S. Y. Shi, *Appl. Surf. Sci.*, 253 (2006) 2132-2137.
27. H. K. Lee, H. Y. Lee and J. M. Jeon, *Surf. Coat. Technol.*, 201 (2007) 4711–4717.
28. P. Montoya, T. Marín, A. Echavarría and J. A. Calderón, *Int. J. Electrochem. Sci.*, 8 (2013) 12566 – 12579.
29. P. Cojocar, A. Vincenzo and P. L. Cavallotti, *J. Solid State Electrochem.*, 9 (2005) 850–858.
30. Y. N. Gou, W. J. Huang, R. C. Zeng and Y. Zhu, *Trans. Nonferrous Met. Soc. China*, 20 (2010) 674–678.
31. M. S. Ali Eltoun, A. M. Baraka, M. M. Saber and A. H. ELfatih, *International Journal of Multidisciplinary Sciences and Engineering*, 2 (2011) 1–6.
32. R. K. Saha, M. Mohamed and T. I. Khan, Wiley: *Processing and Properties of Advanced Ceramics and Composites III: Ceramic Transactions*, 225 (2011) 41–50.
33. E. C. Lee and J. W. Choi, *Surf. Coat. Technol.*, 148 (2001) 234–240.
34. V. Uskoković, *J. Dispers. Sci. Technol.*, 33 (2012) 1762–86.
35. P. Narasimman, M. Pushpavanam and V. M. Periasamy, *Appl. Surf. Sci.*, 258 (2011) 590-598.
36. C. Jackson and A. T. Kuhn, *Elsevier Publishing Amsterdam*, 1971, London, New York.
37. R. Juškėnas, I. Valsiūnas, V. Pakštas and R. Giraitis, *Electrochimica. Acta.*, 54 (2009) 2616–2620.
38. O. Younes-Metzler, L. Zhu and E. Gileadi, *Electrochimica. Acta.*, 48 (2003) 2551–2562.
39. O. Younes, L. Zhu, Y. Rosenberg, Y. Shacham-Diamand and E. Gileadi, *Langmuir*, 17 (2001) 8270–8275.
40. O. Younes and E. Gileadi, *J. Electrochem. Soc.*, 149 (2002) C100–C111.
41. N. Eliaz, T. M. Sridhar and E. Gileadi, *Electrochimica. Acta.*, 50 (2005) 2893–2904.
42. O. Younes and E. Gileadi, *Electrochem. Solid-State Lett.*, 3 (2000) 543–545.
43. O. Younes, L. Zhu, Y. Rosenberg, Y. Shacham-Diamand and E. Gileadi, *Langmuir*, 17 (2001) 8270–8275.
44. B. Han and X. Lu, *Surf. Coat. Technol.*, 203 (2009) 3656–3660.

45. J. Li, Y. Sun, X. Sun and J. Qiao, *Surf. Coat. Technol.*, 192 (2005) 331–335.
46. Y. H. Ahmad, J. Tientong, M. Nar, N. D'Souza, A. M. A. Mohamed and T. D. Golden, *Surf. Coat. Technol.*, 259 (2014) 517–525.
47. J. Li, Y. Sun, X. Sun and J. Qiao, *Surf. Coat. Technol.*, 192 (2005) 331– 335.
48. K. H. W. Seah, M. Krishna, V. T. Vijayalakshmi and J. Uchil, *Corros. Sci.*, 44 (2002) 917–925.
49. S. C. Sharma, K. H. W. Seah, B. M. Satish and B. M. Girish, *Corros. Sci.*, 39 (1997) 2143–2150.
50. J. F. McIntyre, R. K. Conrad and S. L. Golledge, *Corrosion*, 46 (1990) 902-905.
51. Y. Yao, S. Yao, L. Zhang and H. Wang, *Mater. Lett.*, 61 (2007) 67–70.
52. H. Mazaheri and S. R. Allahkaram, *Appl. Surf. Sci.*, 258 (2012) 4574–4580.

© 2016 The Authors. Published by ESG ([www.electrochemsci.org](http://www.electrochemsci.org)). This article is an open access article distributed under the terms and conditions of the Creative Commons Attribution license (<http://creativecommons.org/licenses/by/4.0/>).